THE ASTROPHYSICAL JOURNAL, 488:642–651, 1997 October 20

DYNAMICS OF ORBITS AND LOCAL GAS STABILITY IN A LOPSIDED GALAXY

CHANDA J. JOG
Department of Physics, Indian Institute of Science, Bangalore 560012, India; cjjog@physics.iisc.ernet.in
Received 1996 October 14; accepted 1997 May 28

ABSTRACT

We study the dynamics of particles in closed orbits in a galactic disk perturbed by a lopsided halo potential. The underlying potential in a large fraction of spiral galaxies is now believed to have this form. The orbits are solved via first-order epicyclic theory, and the azimuthal variation in the effective surface density is obtained for an exponential disk. The results are obtained first for a flat rotation curve and then for a general power-law rotation curve. These are shown to be valid for both stars and gas in the inner (optical) region of a galaxy because both respond to the same lopsided potential and have comparable disk scale lengths. The results are applied to external lopsided galaxies.

An orbit is shown to be elongated along the minimum in the lopsided potential. The net rotational velocity is highest at the minimum radial extent of the orbit. The perturbation parameter for the lopsided potential $\epsilon_{\rm lop}$, is obtained as a function of the observed fractional amplitude of the $m = 1$ azimuthal Fourier component of the surface brightness and the radius. The ellipticity of isophotes is shown to be higher by at least a factor of 4 compared to $\epsilon_{\rm lop}$. This explains why the phenomenon of lopsidedness is so commonly detected. It also means that even visually strongly lopsided galaxies have a fairly axisymmetric potential, with a small $\epsilon_{\rm lop} < 0.1$. The effective disk surface density is highest along the maximum in the lopsided potential, and there is an underdense region in the opposite direction. The maximum increase in the surface density is high $\sim$35%–50%, for strongly lopsided galaxies.

We obtain the local stability parameter $Q_{\rm lop}$ in a lopsided galaxy and show that its values for gas are significantly lowered compared to the axisymmetric case in the overdense region. This is argued to result in an enhanced formation of massive stars which then result in H II regions. Thus we can naturally explain the observed azimuthal asymmetry in the distribution of molecular hydrogen gas and H II regions in the lopsided galaxies such as M101.

Subject headings: galaxies: individual (M101) — galaxies: ISM — galaxies: kinematics and dynamics — galaxies: spiral — galaxies: structure — stars: formation

1. INTRODUCTION

1.1. *Lopsided Galaxies: Background*

It has been known for a long time that the light distribution in disks of spiral galaxies is not strictly axisymmetric, as for example in M101 (NGC 5457) (Arp 1966) or in NGC 1637 (Sandage 1961). Despite this, however, astronomers have continued largely to ignore this fact and to assume the disks to be axisymmetric since this simplifies the dynamics of the system. This issue was first discussed in detail by Baldwin, Lynden-Bell, & Sancisi (1980; hereafter BLS), who studied galaxies which had highly asymmetric spatial extent of atomic hydrogen gas distributions in the outer regions in the two halves of a galaxy. They assigned the apt title of *lopsided* to such galaxies. This asymmetry may be fitted by azimuthal $m = 1$ Fourier component, that is, by a cos ϕ distribution, where ϕ is the azimuthal angle in the plane of the disk (e.g., Bosma, Goss, & Allen 1981). Based on a global H I profile mapping of a much larger sample of galaxies, Richter & Sancisi (1994) show that the global H I profile is well correlated with an asymmetry in the spatial distribution of H I. They find that a large fraction of disks studied show an asymmetric distribution of H I. Recent near-IR observations have now revealed an $m = 1$ small-amplitude distribution also in the old stars in a large number of spiral galaxies (Block et al. 1994; Rix & Zaritsky 1995, hereafter RZ). For example, nearly 30% of the sample by RZ shows a 20% or larger fractional amplitude for the $m = 1$ component. This result has been confirmed for a larger sample of 60 field spiral galaxies by Zaritsky & Rix (1997). The RZ sample was chosen so that there is no clear correlation between the galaxies included and their disk shapes. Therefore, it appears that the lopsidedness is a general and hence a long-lived phenomenon. Hence, it is interesting to look at various *dynamical effects* for a galactic disk which has a lopsided halo potential as a perturbation imposed on the underlying axisymmetric potential. This is the motivation for the present paper.

The origin of the $m = 1$ disk distribution is not understood well and, in fact, has not received much theoretical attention until recently. Tidal interaction was suggested by Beale & Davies (1969) to explain the origin of the observed H I asymmetry in M101. However, there are several lopsided galaxies, e.g., NGC 2841, that do not have any close companion, as pointed out by BLS. Instead, BLS proposed a kinematical model where a slow differential shearing of initially aligned orbits leads to a long-lived $m = 1$ distribution in the disk. Earn & Lynden-Bell (1966) have shown that the cooperation of orbital streams of stars near resonance can lead to a long-term maintenance of an $m = 1$ pattern, but they do not address its origin. Phookun, Vogel, & Mundy (1993) propose that the $m = 1$ asymmetry in NGC 4254 could be explained as swing amplification in gravitationally coupled stars and gas (as in Jog 1992), where the seed perturbation is provided by an interaction with the infalling gas. Sellwood & Merritt (1994) explain the origin of this distribution as an instability in counterrotating streams of stars. Junqueira & Combes (1996) explain the $m = 1$ spiral feature in *gas* as a gravitational instability. Zaritsky & Rix (1997) have proposed an accretion of a small

galaxy as the cause of this phenomenon. In this paper, we do not deal with the issue of the origin of the lopsided potential, but rather assume that it arises due to a perturbation in the halo and that it is a long-lived phenomenon lasting for times greater than dynamical timescales, and we study the disk response to this potential.

1.2. *Asymmetric Distribution of Gas and* H II *Regions*

The lopsided galaxies such as M101 show a clear asymmetry in the optical distribution which is more elongated along the southwest direction than the northeast (Arp 1966). In the inner parts of the galaxy, the peaks in the distribution of atomic hydrogen gas coincide quite well with the optical/spiral features (Rogstad 1971; Allen 1975).

We point out that, in addition, the CO observations of M101 also show more extended molecular hydrogen in the southwestern region (Solomon et al. 1983, see their Fig. 2; Kenney, Scoville, & Wilson 1991, see their Fig. 1). Richmond & Knapp (1986) find that the H_2 distribution in NGC 4565 is asymmetric and has a higher radial extent toward the northwest side of the galaxy. This coincides with the behavior of atomic hydrogen gas in inner regions of this galaxy (Rupen 1991). IC 342 (Sage & Solomon 1991) shows a mild asymmetry in the distribution of molecular hydrogen gas, which is more extended along the northeast arm in the galaxy. NGC 628 (M74) also exhibits an asymmetric distribution of H_2, which is more extended along the southwest on the major axis (Adler & Liszt 1989), and also is seen in the two-dimensional map by Sakamoto & Hasegawa (1997). The galaxy M51, which has one arm (along the northeast) longer than the other and is lopsided at all radii in the old stellar component (Rix & Rieke 1993), also shows an asymmetric H_2 distribution (Lord & Young 1990).

It is also well known that there are more and brighter H II regions in the southwestern parts of M101 (Sandage 1961; Allen 1975; Bosma et al. 1981). The K'-band (2.1 μm) imaging study by Block et al. (1994) shows that the H II regions in the lopsided galaxies are asymmetrically distributed, for example a larger number of H II regions in NGC 2997 are along the southern arm.[1]

One aim of this paper is to explain these puzzles of asymmetric distribution of gas and H II regions in lopsided galaxies. We specifically consider gas in the optical region of galaxies so that the stars and gas will experience and respond to the same lopsided potential. Thus we study the asymmetry in the molecular hydrogen gas and in the atomic hydrogen gas located in the inner/optical regions of the disk. We do not consider the extended atomic hydrogen gas since it will respond to the lopsided potential in external regions, which may not have any correlation with the asymmetry in potential in the inner regions; this point is discussed in detail in § 4.2.

1.3. *Outline*

We first study the dynamics of closed orbits in a perturbation lopsided potential via first-order epicyclic theory and obtain the azimuthal variation in the effective surface density for an exponential disk. These results are shown to be valid for stars and gas in the inner (optical) regions, because both respond to the same lopsided potential and have comparable disk scale lengths. The azimuthal variation in gas density is shown to affect the local gas stability, and this leads to an azimuthally asymmetric formation of massive stars and hence H II regions. These results are shown to agree with the observations of lopsided galaxies.

In § 2, the properties of the closed orbits in a $m = 1$ perturbation potential are calculated, and the variation in density with the azimuthal angle is obtained. In § 3, the criterion for local stability in a lopsided potential is obtained, and the effect on gas stability and the resulting asymmetric star formation is studied. A few general points are discussed in § 4. The conclusions of this paper are summarized in § 5.

2. DYNAMICS OF ORBITS IN A LOPSIDED POTENTIAL

2.1. *Calculation of Closed Orbits*

We obtain the closed loop orbits in a galactic disk when an azimuthally symmetric disk potential is perturbed by a small lopsided potential. We take the net potential ψ at a given radius R to be a sum of the unperturbed potential, $\psi_0(R)$, and the first-order (small) perturbation potential, $\psi_{\rm lop}(R)$, so that

$$\psi(R) = \psi_0(R) + \psi_{\rm lop}(R) , \tag{1}$$

where

$$\psi_{\rm lop}(R) = \psi_{\rm pert}(R) \cos \phi . \tag{2}$$

Here $\psi_{\rm lop}(R)$ is taken to be nonrotating; this assumption is justified since this potential is assumed to arise due to a perturbation in the halo (§ 1).

A perturbed orbit around the initial circular orbit at R_0 may be written as $R = R_0 + \delta R$ and $\phi = \phi_0 + \delta\phi$. Here ϕ is the azimuthal angle in the galactic disk plane in the cylindrical coordinate system and $\phi_0 = \Omega_0 t$, where Ω_0 is the circular rotation speed at R_0 given by

$$R_0 \Omega_0^2 = \left.\frac{d\psi_0}{dR}\right|_{R_0} . \tag{3}$$

Using the first-order epicyclic theory (Rohlfs 1977; Gerhard & Vietri 1986), the equations of motion for δR and $\delta\phi$ are

$$\frac{d^2\,\delta R}{dt^2} = -\delta R\left(3\Omega_0^2 + \left.\frac{d^2\psi_0}{dR^2}\right|_{R_0}\right) - \left[\frac{2\psi_{\rm pert}(R_0)}{R_0} + \left.\frac{d\psi_{\rm pert}}{dR}\right|_{R_0}\right] \cos\phi_0 , \tag{4}$$

$$R_0\,\frac{d^2\,\delta\phi}{dt^2} + 2\Omega_0\,\frac{d\,\delta R}{dt} = \frac{\psi_{\rm pert}(R_0)}{R_0} \sin\phi_0 . \tag{5}$$

The first term in the parentheses on the right-hand side of equation (4) is the square of the standard first order epicyclic frequency, κ, at R_0. Thus, as expected, equations of motion for the perturbed motion contain the standard epicyclic term and an extra term due to the lopsided potential. From the theory of a forced oscillator (e.g., Symon 1960), the above equations may be solved to yield the following solution for the closed orbits:

$$\delta R = \left\{-\left[\frac{2\psi_{\rm pert}(R_0)}{R_0} + \left.\frac{d\psi_{\rm pert}}{dR}\right|_{R_0}\right] \Big/ (\kappa^2 - \Omega_0^2)\right\} \cos\Omega_0 t . \tag{6}$$

[1] It is interesting and indicative of the common occurrence of lopsidedness that even NGC 2997 which is often referred to as a typical spiral galaxy—for example, see the jacket illustration of Binney & Tremaine (1987)—exhibits lopsidedness (see Block et al. 1994).

So far the calculation is valid for a general ψ_0 and $\psi_{\rm pert}$. In this paper we choose ψ_0, the unperturbed potential, to be a logarithmic potential of the form

$$\psi_0(R) = V_c^2 \ln R . \tag{7}$$

This is applicable for a region of flat rotation, with V_c being the constant rotational velocity. This choice simplifies the calculation and yet represents the behavior over a large fraction of the disk in a typical spiral galaxy (Bosma 1978; Rubin, Ford, & Thonnard 1978). This potential has been used for studies of perturbed orbits in an elliptical potential ($m = 2$) by Franx & de Zeeuw (1992), and Kuijken (1993). The choice of ψ_0 as in equation (7) gives $\kappa^2 = 2\Omega_0^2$, as expected for a region of flat rotation curve. We treat the case of a generalized rotation curve in § 2.5.

The lopsided potential $\psi_{\rm lop}$ (eq. [2]) is chosen to have the form

$$\psi_{\rm lop}(R) = \psi_{\rm pert}(R) \cos \phi = V_c^2 \epsilon_{\rm lop} \cos \phi , \tag{8}$$

where $\epsilon_{\rm lop}$ is a small perturbation parameter. Using this form of the perturbation potential, equation (6) reduces to

$$\delta R = -2R_0 \epsilon_{\rm lop} \cos \phi_0 .$$

Thus the net radius is given as

$$R = R_0 + \delta R = R_0(1 - 2\epsilon_{\rm lop} \cos \phi_0) . \tag{9}$$

Hence V_R, the perturbed velocity along the radial direction, is given as

$$V_R = 2V_c \epsilon_{\rm lop} \sin \phi_0 . \tag{10}$$

On substituting the solution for δR from equation (9) in equation (5) for the ϕ component of the equation of motion and integrating it, we obtain the solution for the perturbed velocity δV_ϕ. The net velocity along the azimuthal direction is

$$V_\phi = V_c + \delta V_\phi = V_c(1 + 3\epsilon_{\rm lop} \cos \phi_0) . \tag{11}$$

Hence the equations of motion for the perturbed, closed orbits in the lopsided potential are given by equations (9)–(11). Thus an orbit is elongated along $\phi = 180°$, that is, along the minimum of the lopsided potential, whereas the orbit is shortened along $\phi = 0°$. The net rotation velocity is highest at $\phi = 0°$, see § 2.3 for observational implications.

When the test particle has a nonzero random velocity, the general solution for δR (eq. [9]) has an additional term $[(\langle V_r^2 \rangle^{1/2})/\kappa] \cos \kappa t$, where $\langle V_r^2 \rangle^{1/2} = c$ is the rms one-dimensional velocity dispersion of the particles. The resulting orbit is not closed in this case. In § 2.2 we show that the effect of random motion may be ignored while studying the isophotal shapes.

2.2. *Isophotal Shapes in an Exponential Disk*

We next calculate $\epsilon_{\rm lop}$, the perturbation parameter for the lopsided potential (eq. [8]) as a function of the isophotal shapes, and examine the physical consequences of the results. Consider the unperturbed surface brightness to have an exponential dependence on radius as observed in a typical galactic disk (Freeman 1970; Mihalas & Binney 1981). Assuming as usual a constant mass to light ratio, this gives the unperturbed surface density $\mu_{\rm un}$ of the stellar disk, to be:

$$\mu_{\rm un}(R) = \mu_0 \exp [-(R/R_{\rm exp})] , \tag{12}$$

where μ_0 is the central extrapolated surface density and $R_{\rm exp}$ is the exponential disk scale length. For a disk with a lopsided ($m = 1$) distribution, the fractional amplitude of the $m = 1$ azimuthal Fourier component of the surface brightness is given as $A_1/A_0 = \Delta\mu/\langle\mu\rangle$ where $\langle\mu\rangle$ is the azimuthal average. For an exponential disk, this can be shown to be equal to

$$\frac{A_1}{A_0} = \left| -\frac{\Delta R}{R} \frac{R}{R_{\rm exp}} \right| . \tag{13}$$

This results in a positive definite value for A_1/A_0. Here $\Delta R/R$ is the distortion in the isophote, and is related to $\epsilon_{\rm iso}$, the ellipticity of an isophote at R, as follows:

$$\epsilon_{\rm iso} = 1 - R_{\rm min}/R_{\rm max} = 2(\Delta R/R) , \tag{14}$$

where $R_{\rm min}$ and $R_{\rm max}$ are the minimum and maximum extents of an isophote respectively. Note that here both $R_{\rm min}$ and $R_{\rm max}$ are along the same axis, unlike the standard definition of ellipticity where they are along directions that are normal to each other. We adopt this nonstandard notation for the sake of continuity with that used by RZ in their observational determination of $\epsilon_{\rm iso}$.

From equations (13) and (14), A_1/A_0 is obtained in terms of $\epsilon_{\rm iso}$ as follows:

$$\frac{A_1}{A_0} = \frac{\epsilon_{\rm iso}}{2} \frac{R}{R_{\rm exp}} . \tag{15}$$

Since the orbital velocity changes along the perturbed orbit, the associated surface density also changes as a function of the angle ϕ. The changes for particles on these orbits are governed by the equation of continuity:

$$\frac{\partial}{\partial R} [R\mu(R, \phi)V_R(\phi)] + \frac{\partial}{\partial \phi} [\mu(R, \phi)V_\phi(\phi)] = 0 . \tag{16}$$

Now the effective surface density for an exponential disk with perturbed orbits in a lopsided disk potential (as given by eqs. [9]–[11]) may be written as

$$\mu(R, \phi) = \mu_0 \exp \left[-\frac{R}{R_{\rm exp}} \left(1 - \frac{\epsilon_{\rm iso}}{2} \cos \phi \right) \right] . \tag{17}$$

On solving together the equations of the perturbed motion (eqs. [9]–[11]), the continuity equation (eq. [16]), and the equation for the effective surface density (eq. [17]), we obtain the relation between $\epsilon_{\rm iso}$ and $\epsilon_{\rm lop}$ at a given radius R,

$$\frac{\epsilon_{\rm iso}}{\epsilon_{\rm lop}} = 4\left(1 + \frac{R_{\rm exp}}{2R} \right) , \tag{18}$$

where $R \geq R_{\rm exp}$ since the calculation of loop orbits (§ 2.1) is valid for this range (see RZ). Note that the ellipticity of isophotal contours is *higher by a least a factor of* 4 compared to $\epsilon_{\rm lop}$ (eq. [18]). The large value of the ratio $\epsilon_{\rm iso}/\epsilon_{\rm lop}$ makes the detection of lopsidedness easier, and this explains why a large fraction of spiral galaxies are observed to be lopsided.

The maximum and minimum lopsided potentials occur along $\phi = 0°$ and $\phi = 180°$, respectively (see eq. [8]), that is, along the same axis but in opposite directions. Despite this, if one were to define the ellipticity of equipotentials for the

lopsided case, say $\epsilon'_{\rm lop}$ (in analogy with the nonstandard definition of $\epsilon_{\rm iso}$ as discussed above), then it can be shown that $\epsilon'_{\rm lop}$ is equal to $2\epsilon_{\rm lop}$. From equation (18) we can thus see that the ellipticity of the isophotes is higher by at least a factor of 2 compared to the ellipticity of the lopsided potential. Thus, the isophotal contours are more elongated by at least a factor of 2 compared to the equipotential contours.

From equations (15) and (18), $\epsilon_{\rm lop}$ is obtained in terms of A_1/A_0 to be

$$\epsilon_{\rm lop} = \frac{A_1/A_0}{2[(1/2) + (R/R_{\rm exp})]} . \quad (19)$$

While obtaining $\epsilon_{\rm lop}$ from the isophotal shapes, we have ignored the effect of the random motion of the stars. This is justified because inclusion of random motion in the problem would lead to an addition of a term in the resulting perturbed radius as discussed at the end of § 2.1. This would only change the resulting values of the isophotal ellipticity $\epsilon_{\rm iso}$ by a factor $\sim[1 - (\langle V_r^2\rangle/V_c^2)]$ (e.g., RZ), and the second term in this expression can be ignored in the limit of small velocity dispersion $\langle V_r^2\rangle^{1/2} = c \ll V_c$. This is true in a typical galactic disk since c is observed to be much less than V_c (Mihalas & Binney 1981).

Using equations (18) and (19), we next obtain the resulting values of $\epsilon_{\rm lop}$ and $\epsilon_{\rm iso}$ as functions of $R/R_{\rm exp}$ for the observed values of A_1/A_0. The mean observed value of A_1/A_0 for the galaxies in the RZ sample is $A_1/A_0 = 0.14$, while 30% of their sample shows larger values of $A_1/A_0 \geq 0.19$–0.2, as measured at $R/R_{\rm exp} = 2.5$. Below this radius, the A_1/A_0 values are observed to be much smaller, and they increase beyond this radius. For the typical value of $A_1/A_0 = 0.14$, we get the resulting $\epsilon_{\rm lop} = 0.02$, and $\epsilon_{\rm iso} = 0.11$. The higher value of $A_1/A_0 = 0.2$ gives $\epsilon_{\rm lop} = 0.03$, and $\epsilon_{\rm iso} = 0.16$. The observed increase in A_1/A_0 with radius results in a higher perturbation potential $\epsilon_{\rm lop}$ at larger radii in a galactic disk.

We would like to apply the above results to visually extremely lopsided galaxies such as M101 and NGC 1637 (Sandage 1961). Unfortunately, these have not been included in the samples of RZ or Zaritsky & Rix (1997). For such highly lopsided galaxies, a higher value of A_1/A_0, say, ~ 0.3–0.4, may be a reasonable choice. Note that even these can still be represented by a small value of $\epsilon_{\rm lop} \leq 0.07$ because of the large value of the ratio of $\epsilon_{\rm iso}/\epsilon_{\rm lop}$ (eq. [18]). Thus, the net gravitational potential in the disk is not very far from axisymmetry; hence, the first-order epicyclic theory used in § 2.1 to derive the orbits would be applicable for such cases. This is also the physical reason why despite the visual asymmetry such galaxies are dynamically robust.

For the typical value of $\epsilon_{\rm iso} = 0.11$ (at $A_1/A_0 = 0.14$) as calculated above (eq. [15]), the axis ratio of an isophote, $R_{\rm min}/R_{\rm max}$ (see eq. [14]) is 0.89, which is substantially different from a circular shape. For a much stronger lopsided case with say $A_1/A_0 = 0.3$ or 0.4, the axis ratio would be even smaller = 0.76 and 0.68 respectively, giving *the isophotes a distinctly egg-shaped oval appearance.*

For a particular isophote, the term in brackets in equation (17) is a constant. This formally defines the parametric form of an isophote. Hence it can be seen that $R_{\rm min}$ of an isophote occurs along $\phi = 180°$, while $R_{\rm max}$ occurs along $\phi = 0°$. This is opposite to the behavior of an individual orbit (see eq. [9] and the discussion in § 2.1). Thus, in an exponential disk, the isophotes are elongated in a direction opposite to the elongation in the orbits. The isophotes are elongated along the same direction where the maximum effective surface density occurs (see § 2.7 for details). This is true for any centrally concentrated galactic disk.

2.3. *Velocity Components*

The net rotation velocity is given by equation 11 and is highest at $\phi = 0°$, along the maximum in the lopsided potential, that is, at the minimum radial extent of an orbit. This could be important in explaining the observed asymmetry of rotation curves in lopsided galaxies (e.g., Mihalas & Binney 1981) and will be studied in a future paper.

Equation (10) denotes the coherent radial velocity for orbits in a lopsided potential; this is dependent on the angle ϕ in a disk and has a maximum magnitude at $\phi = 90°$ and 270°. The typical rms value of this streaming velocity is obtained by averaging equation (10) over the azimuthal angles and using equation (19), it is written as follows:

$$\langle V_R^2\rangle^{1/2} = 2^{1/2} V_c \epsilon_{\rm lop} = \frac{(A_1/A_0)V_c}{2^{1/2}[(1/2) + (R/R_{\rm exp})]} . \quad (20)$$

This is the quantity determined from observations of a sample of galaxies of arbitrary orientations. For a typical value of $V_c = 220$ km s^{-1} and $A_1/A_0 = 0.14$ at $R = 2.5R_{\rm exp}$ (see § 2.2), this gives $\langle V_R^2\rangle^{1/2} = 7.3$ km s^{-1}. For stronger lopsided cases, with, say, $A_1/A_0 = 0.2$–0.3, the resulting streaming motion is 10–16 km s^{-1}. This is $\sim 50\%$ of the radial stellar random velocity dispersion, which we have ignored here for simplicity (§ 2.2).

2.4. *Comparison with Earlier Work*

The equations of motion for closed orbits in a lopsided potential were obtained by RZ. However, their results are not correct and are also not internally consistent. They give (see eqs. [20]–[22] from RZ):

$$R = R_0[1 - (\epsilon_{\rm lop}/2)\cos\phi] , \quad V_R = -V_c(\epsilon_{\rm lop}/2)\sin\phi ,$$
$$V_\phi = V_c[1 + (\epsilon_{\rm lop}/2)\cos\phi] . \quad (21)$$

The above expression for R is correct only if the perturbation potential is taken to be $V_c^2(\epsilon_{\rm lop}/4)\cos\phi$ and not $V_c^2(\epsilon_{\rm lop}/2)\cos\phi$ as they state at the end of their § 4. Further, for the above result of R, the corresponding V_R should have a plus sign (+) ahead and not a minus sign (−), and the term in the parentheses containing $\epsilon_{\rm lop}$ in the expression for V_ϕ should have a factor of 3/2 before it. Thus their resulting expressions for $\epsilon_{\rm lop}$ and the rms radial streaming velocity, $\langle V_R^2\rangle^{1/2}$, are not correct. For their choice of $V_c = 200$ km s^{-1}, $A_1/A_0 = 0.11$, and at $R = 2.5R_{\rm exp}$, the correct value of the rms streaming velocity from our equation (20) is 5.2 km s^{-1}, which is smaller than the RZ value of 7.4 km s^{-1}. We wish to point out and correct these errors in the pioneering work by RZ on the nonaxisymmetric amplitudes in stars. We use the observed values of A_1/A_0 from RZ to obtain results for a typical galaxy (see §§ 2.2, 2.6, and 2.7).

2.5. *Results for a General Rotation Curve*

Here we extend the results for closed orbits in a lopsided potential for an exponential disk (§§ 2.1, 2.2) to the case of a general rotation curve given by

$$V = V_c(R/R_0)^\alpha , \quad (22)$$

where V_c is the circular velocity at R_0, and α is a non-zero small number (<1) and is the logarithmic slope of the rotation curve. This form represents the general rotation curve

in the disk of a typical spiral galaxy (Schechter 1996, Casertano & Van Gorkom 1991). This case is worth studying since the A_1/A_0 values are observed to increase at large radial distances (see § 2.2), where the rotation curve may not be flat. The corresponding unperturbed potential, ψ_0, is given by (see, e.g., Kuijken & Tremaine 1994):

$$\psi_0 = (V_c^2/2\alpha)(R/R_0)^{2\alpha} . \quad (23)$$

We assume the perturbation potential in this case to be

$$\psi_{\rm lop}(R) = V^2 \epsilon_{\rm lop} \cos \phi , \quad (24)$$

where V is defined by equation (22). This is analogous to the choice (eq. [8]) for the flat rotation curve. Following an analysis similar to that in § 2.1, it can be shown that a closed orbit in this case is given by

$$R = R_0[1 - 2\epsilon_{\rm lop}(1 - \alpha) \cos \phi_0] ,$$
$$V_R = +2V_c \epsilon_{\rm lop}(1 - \alpha) \sin \phi_0 ,$$
$$V_\phi = V_c\{1 + 3\epsilon_{\rm lop}[1 - (4/3)\alpha] \cos \phi_0\} . \quad (25)$$

Next, following the analysis similar to that in § 2.2, it can be shown that for this general case, $\epsilon_{\rm iso}$ is related to $\epsilon_{\rm lop}$ as follows:

$$\frac{\epsilon_{\rm iso}}{\epsilon_{\rm lop}} = 4\left[(1 - \alpha) + \frac{R_{\rm exp}}{2R}(1 - 2\alpha)\right] . \quad (26)$$

The effective surface density is again given by equation (17) as before, except that the relation between $\epsilon_{\rm iso}$ and $\epsilon_{\rm lop}$ is now specified by equation (26). Combining this with equation 15 for A_1/A_0, we get

$$\epsilon_{\rm lop} = (A_1/A_0)/2[(\tfrac{1}{2} - \alpha) + (R/R_{\rm exp})(1 - \alpha)] . \quad (27)$$

Consider a region of slowly increasing rotation curve in a galactic disk so that α is greater than 0. This is observed to be the case in the outer regions of late-type spiral galaxies (Bosma 1978), and particularly for the Magellanic-type dwarf irregular galaxies (Casertano & Van Gorkom 1991). Comparing equations (9) and (25), and equations (18) and (26), it can be seen that for a given $\epsilon_{\rm lop}$ value, the maximum radial extent of an orbit along $\phi = 180°$, and also the ratio of $\epsilon_{\rm iso}/\epsilon_{\rm lop}$, are slightly smaller in this case than for a flat rotation curve. However, this effect is somewhat compensated by the increase in the value of $\epsilon_{\rm lop}$ with radius as shown in § 2.2.

In contrast, the rotation curve is observed to decrease at large radii in some cases, as for example in a few interacting galaxies and especially in galaxies in denser environments as in clusters of galaxies (Rubin, Whitmore, & Ford 1988) and in the case of large, early-type galaxies (Casertano & Van Gorkom 1991). In this case, $\alpha < 0$; hence, the maximum radial extent and the ratio of $\epsilon_{\rm iso}/\epsilon_{\rm lop}$ are higher than for a flat rotation curve.

2.6. *Dependence on Phase, $\phi_{\rm lop}(R)$, of the Lopsided Potential*

We define the phase of the lopsided potential at a given radius R to be $\phi_{\rm lop}(R)$. In equation (8) we have set this equal to 0°. This is always valid for a given radius since by a suitable transformation of coordinates one can effectively set this phase to be 0°. The same is true if $\phi_{\rm lop}(R)$ is constant with radius. In this case, the results in §§ 2.1–2.3, and § 2.5 are valid. The observations seem to support this assumption for *strongly lopsided galaxies*, as we discuss later in this subsection.

If, on the other hand, $\phi_{\rm lop}(R)$ shows a significant variation with radius, then the definition of lopsided potential (eq. [8]) has to be modified as follows:

$$\psi_{\rm lop}(R) = V_c^2 \epsilon_{\rm lop} \cos [\phi - \phi_{\rm lop}(R)] . \quad (28)$$

The resulting expressions for the equations of motion (eqs. [9]–[11], and [25]), and the effective surface density (eq. [17]), will then be modified in a straightforward way so that the angle in the trigonometric terms will now be $\phi - [\phi_{\rm lop}(R)]$ instead of being ϕ as before. On comparing the modified equation (17) with the standard Fourier expansion (see, e.g., RZ), it can be seen that the phase of the first azimuthal Fourier component, $\phi_1(R)$, is equal to $\phi_{\rm lop}(R)$,

$$\phi_1(R) = \phi_{\rm lop}(R) . \quad (29)$$

Observations of lopsided galaxies show that $\phi_1(R)$ is remarkably constant in the outer optical regions where the galaxy is lopsided [see the plot of $\phi_1(R)$ vs. radius; Fig. 2 of RZ] for the six out of 18 galaxies with a high measured lopsidedness ($A_1/A_0 \geq 0.19$ for $R \geq 2.5R_{\rm exp}$), such as NGC 1325A, NGC 2485, and NGC 6814. The one exception is NGC 7309, which has an abrupt change in $\phi_1(R)$ between 2 and 3 times $R_{\rm exp}$; this could be related to its being a three-armed galaxy. In contrast, the galaxies in the RZ sample with lower A_1/A_0 values (≤ 0.05); such as NGC 1642 and NGC 7742, show more variation in ϕ_1 with radius. NGC 1703, despite being fairly strongly lopsided (with $A_1/A_0 = 0.17$), shows an abrupt change in $\phi_1(R)$ in this radial region.

The constancy of the phase $\phi_1(R)$ means that $\phi_{\rm lop}(R)$ is also constant with radius (see eq. [29]). Therefore, the results in §§ 2.1–2.5 are valid as they are for strongly lopsided galaxies. We have assumed that the lopsided potential originates in the halo (see §§ 1.1 and § 4.1), and physically it is reasonable that the distortion in the spheroidal dark matter halo would be a global one, and hence the phase of the potential would not vary with radius. In any case, for the sake of completeness, we discuss next the resulting changes in the isophotes, and the changes in star formation (see § 3.3), that arise if the phase $\phi_{\rm lop}(R)$ were to vary with the radius. Note that $\phi_1(R)$ denotes the position angle of the major axis of an isophote (e.g., Mihalas & Binney 1981). If the observed phase $\phi_1(R)$, is constant with radius as is typically observed, then the isophotes are seen to be aligned with their major axes all lying along the same direction. Thus, the isophotal shapes will have aligned egg-shaped contours with the shapes as discussed at the end of § 2.2. This seems to describe the overall optical appearance of lopsided galaxies such as M101 and NGC 1637 (Sandage 1961). If, on the other hand, $\phi_1(R)$, and hence $\phi_{\rm lop}(R)$, in a galaxy shows a variation with radius, then the $R_{\rm max}$ of an isophote will occur at different angles at different radii, as can be seen from a modified equation (17) with ϕ replaced by $\phi - \phi_{\rm lop}(R)$. Hence, the isophotes will then show a prominent one-armed spiral structure in the galaxy. This is applicable for galaxies such as M51 or NGC 2997 (Block et al. 1994) which show one prominent spiral arm.

2.7. *Fractional Change in Surface Density*

The ratio of the effective surface density for the perturbed orbits in a lopsided potential (eq. [17]) and the unperturbed surface density (eq. [12]), is taken to define f_μ, the fractional change in the surface density, at a given point (R, ϕ) in the disk, and is given by the following simple analytical function:

$$f_\mu \equiv \exp [(A_1/A_0) \cos \phi] , \quad (30)$$

where A_1/A_0 is related to ϵ_{lop} via equation (19) for a flat rotation curve and via equation (27) for a general case. The above assumes a constant phase $\phi_{lop}(R)$ as is observed for strongly lopsided galaxies (§ 2.6). If $\phi_{lop}(R)$ varies with radius as observed for weakly lopsided galaxies, then ϕ in equation (30) would be replaced by $\phi - \phi_{lop}(R)$.

In Figure 1, f_μ, the fractional change in the surface density is plotted as a function of the azimuthal angle ϕ, for the values of $A_1/A_0 = 0.1$, 0.2, 0.3, and 0.4. First, we note that there is an overdensity ($f_\mu > 1$) for $\phi = 0°$–$90°$, and $\phi = 270°$–$360°$, while there is an underdensity ($f_\mu < 1$) for the other half of the disk, namely from $\phi = 90°$ to $270°$. Thus the most underdense and the overdense regions are located at 180° with respect to each other. Second, the resulting maximum increase in surface density at $\phi = 0°$ is high for strongly lopsided galaxies, equal to 35% and 50% for $A_1/A_0 = 0.3$ and 0.4, respectively.

The maximum of the effective disk density occurs at $\phi = 0°$, which is along the maximum of the lopsided potential (see eq. [8]). We note that the potential corresponding to this disk response would be a minimum along $\phi = 0°$, at the region of maximum surface density (Binney & Tremaine 1987). Thus the potential corresponding to the disk response is *anticorrelated* with the imposed lopsided halo potential. This means that the orbits in a lopsided galaxy do not self-support the potential that they arise from. This result has been shown for a general even-m Fourier component for a disk of logarithmic potential by Kuijken (1993); also see Rix (1996) for the $m = 2$ case). This anticorrelation was stated by RZ for the $m = 1$ case, but they do not give an explicit azimuthal variation in surface density. This effect has been shown to hold for $m = 1$ for the particular case of the Milky Way by Weinberg (1995) (see § 4.1).

An interesting result obtained next is the fraction of the integrated surface density (or mass) in the two halves of the disk. This ratio gives a quantitative measure of the net asymmetry of mass in lopsided galaxies. Assume a constant A_1/A_0 for a certain radial range. For this range of radii, the fraction of total surface density in the overdense regions is obtained by taking a ratio of the integral over the annular region of equation (17) between $\phi = 0°$–$90°$ and $\phi = 270°$–$360°$ to the total integral between $\phi = 0°$–$360°$. This is equal to $0.5 + [2(A_1/A_0)/\pi]$. The integral over the underdense region gives $0.5 - [2(A_1/A_0)/\pi]$. Thus for the typical observed value of $A_1/A_0 = 0.14$, the fraction of net surface density in the overdense regions is 0.59 versus 0.5 for an axisymmetric disk. This increases with A_1/A_0 and is equal to 0.69 or 0.75 for a strongly lopsided galaxy with $A_1/A_0 = 0.3$ or 0.4, respectively. If there is a strong radial variation in the phase $\phi_{lop}(R)$, the hemispheric averages as given above are not applicable.

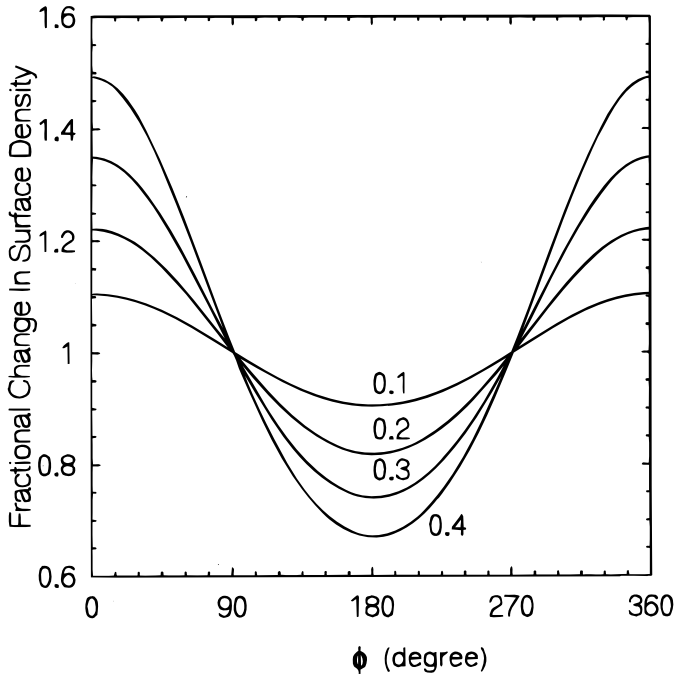

FIG. 1.—Variation in f_μ, the fractional change in the surface density, versus the azimuthal angle ϕ (degree), for the fractional amplitude of the $m = 1$ azimuthal Fourier component of surface brightness $A_1/A_0 = 0.1$, 0.2, 0.3, and 0.4. The maximum overdensity occurs at $\phi = 0°$, along the maximum in the lopsided potential.

2.8. *Validity of Results for Gas*

The results obtained for orbits in §§ 2.1, 2.5, and in 2.6, are valid for both stars and gas located in the same region of a galaxy because they respond to the same lopsided potential. Further, the result for the azimuthal variation in density eq. [17], (§ 2.2), and hence the fractional variation in density (eq. [30], § 2.7) and the isophote shapes (§ 2.6), are valid identically for stars and molecular hydrogen gas since they both have an exponential distribution in the disk with the same disk scale lengths, as shown next. Observations show that on subtracting out the spiral arm contributions, the disk scale length for stars and for molecular gas is measured to have the same value within the errors of measurement as shown for M101 (Solomon et al. 1983; Kenney et al. 1991), for IC 342 (Young & Scoville 1982a), and for NGC 4565 (Richmond & Knapp 1986). The atomic hydrogen gas has a larger scale length (Wevers, van der Kruit, & Allen 1986); hence, for a given ϵ_{lop}, the resulting A_1/A_0 for H I is smaller (eqs. [19] or [27]). Hence, the H I in the inner/optical regions would show smaller overdensity values (eq. [30]), while its variation with the angle ϕ will be the same as for the other components. The gas would survive along the closed orbits since there would be no shocks.

The overdensity in the azimuthal range $\phi = 0°$–$90°$ and $\phi = 270°$–$360°$ (Fig. 1) is shown to significantly decrease the local stability of gas in this region (see § 3.2), resulting in a higher star formation rate (see § 3.3).

Note that, the maximum radial extent of an isophote, occurs along $\phi = 0°$ (see § 2.2), which is where the effective surface density is also the highest (§ 2.7). There is observational evidence for this from the distribution of H_2 gas, and H I gas (in the optical region), in M101 (§ 1.2). This pediction can be checked with future detailed observations of CO and H I in the *inner* regions in other lopsided galaxies, which would yield the azimuthal variation in density.

3. LOCAL GAS STABILITY IN A LOPSIDED GALAXY

Here we study the asymmetric distribution of molecular hydrogen gas (§ 3.1), which is known to be the site of star formation in galaxies. We next obtain the local stability criterion for a lopsided galaxy (§ 3.2), and study the resulting asymmetry in star formation (§ 3.3).

3.1. *The Asymmetry in the Distribution of Molecular Hydrogen Gas*

The distribution of the molecular hydrogen gas in the lopsided galaxies such as M101 and NGC 4565 is clearly

observed to be asymmetric, with a larger radial extent in one-half of a galaxy (§ 1.2). This can be explained naturally on the basis of the closed orbits in a lopsided potential (§ 2) for the molecular clouds. The gas surface density in M101 shows an azimuthal variation in density as predicted (§ 2.8), with the isophotal elongation and the high surface density occurring along the same (southwestern) direction.

In addition, as we argue next, due to gas dynamical effects the fraction of molecular hydrogen gas could increase in regions of overdensity, thus increasing the asymmetry in its distribution. A fraction of the gas which was initially in an atomic hydrogen form would, on getting compressed to a high surface density in the overdense regions (§ 2.7), get converted into a molecular hydrogen form. This follows from the additional self-shielding against UV dissociation provided by the higher surface density region. The minimum atomic hydrogen surface density for which this conversion can occur is $\sim 5\ M_\odot\ \mathrm{pc}^{-2}$ or $6 \times 10^{20}\ \mathrm{H\ cm}^{-2}$, as shown theoretically by Shaya & Federman (1987). This agrees with the observations of gas in galaxies including the Milky Way since any surface density in excess of the above value seems to be seen in a molecular hydrogen form (Solomon et al. 1983; Scoville & Sanders 1987). This threshold is somewhat smaller for the early-type galaxies (Young & Scoville 1991). Thus we predict that the percent asymmetry in the distribution of molecular hydrogen gas would be more than that in the atomic gas in the interior region of a lopsided galaxy (also see § 2.8). The conversion to a molecular hydrogen occurs on timescales (e.g., Duley & Williams 1984) that are shorter than the dynamical or crossing timescale ($\sim 10^8$ yr) in the disk, and hence the above idea of in situ conversion from H I to H_2 for gas above the threshold density is valid.

This effect would be especially significant in large, late-type galaxies, such as for example M101 and NGC 628, which have extended H I distributions going up to a few times the Holmberg radii (Sancisi 1981); hence, the atomic hydrogen density is close to this threshold value over a large radial extent. This conversion would be further helped by the fact that the A_1/A_0 values and hence the values of overdensity (eq. [30]) increase with the radius (§ 2.2).

Most observational results for CO in the literature are presented as azimuthally averaged radial profiles. The results on the asymmetry of gas distribution in the present paper underline the important point that the observational papers should give a full azimuthal distribution or at least values along both sides of the major axis for the H_2 densities. The presence of a bar is an additional source of asymmetry in the distribution of CO as in IC 342, which makes it harder to visually detect the lopsidedness from the CO plots.

Note that the molecular hydrogen is typically contained within half the Holmberg radius (Young et al. 1995), whereas the values for A_1/A_0 are observed to be important beyond $2.5R_{\mathrm{exp}}$ (§ 2.2). The Holmberg radius is about 4 times the disk scale length R_{exp} (Freeman 1970). Hence, we can conclude that H_2 is typically contained within $2R_{\mathrm{exp}}$, and therefore it would not experience the strongest lopsided potential unless the galaxy is large and has an extended CO distribution. This is certainly true in large, late-type galaxies such as M101 and could be one reason why a clear H_2 gas asymmetry is seen in these galaxies. However, in some galaxies such as NGC 4565 (Richmond & Knapp 1986), CO is contained inside of $2.5R_{\mathrm{exp}}$ and yet shows a lopsided distribution. This could mean that the A_1/A_0 values are fairly large even at $R < 2.5R_{\mathrm{exp}}$ in these galaxies. Alternatively, some of this asymmetry could be due to an increased fraction of molecular gas in regions of high surface density as we have argued above.

3.2. *Local Stability Criterion in a Lopsided Galaxy*

We next obtain Q_{lop}, the effective Q criterion for the local stability against axisymmetric gravitational perturbations in a disk perturbed by a lopsided potential. When studying the local stability at a point (R, ϕ), one can consider the standard local, linear perturbation analysis except that now the unperturbed motion is given by equations (10) and (11) for a flat rotation curve, and equation (25) for a general rotation curve. These specify the velocity components along closed orbits at this point. The effective first-order epicyclic frequency in this case, κ_{lop}, can be defined as usual in terms of the Oort constants A' and B' to be

$$\kappa_{\mathrm{lop}} \equiv [-4B'(A' - B')]^{1/2} , \tag{31}$$

where A' and B' are modified Oort constants as valid for the velocity field in a lopsided case. Using the expressions for these for a general velocity field from Kuijken & Tremaine (1994, eq. [8]), we calculate A' and B' for the velocity field in the lopsided case for a general rotation curve (eq. [25]). Keeping the first-order terms in ϵ_{lop} and α, the resulting expression for κ_{lop} is

$$\kappa_{\mathrm{lop}} = \kappa = \left[2^{1/2}\Omega_0\left(1 + \frac{\alpha}{2}\right)\right], \tag{32}$$

where κ is the standard epicyclic frequency for the axisymmetric case. Thus, κ_{lop} is identical to κ since the changes in the velocity field arising in a lopsided case are first order, and since α is small (< 1) (see § 2.5).

On considering axisymmetric perturbations to this region we get the dispersion relation and from that obtain the following expression for Q_{lop}, the local stability parameter for a one-component lopsided disk to be

$$Q_{\mathrm{lop}} = \kappa c/\pi G\mu(R, \phi) , \tag{33}$$

where c is the one-dimensional rms random velocity in the disk. Note that $Q_{\mathrm{lop}} > 1$, $= 1$, and < 1 denotes a stable, marginally stable, and an unstable disk respectively. Writing $\mu(R, \phi)$, the surface density (eq. [17]) in terms of μ_{un}, the unperturbed density (eq. [12]), and f_μ, the fractional change in density (eq. [30]), we get

$$\begin{aligned} Q_{\mathrm{lop}} &= (\kappa c/\pi G\mu_{\mathrm{un}}) \exp\,[-(A_1/A_0)\cos\,\phi] \\ &= Q \exp\,[-(A_1/A_0)\cos\,\phi] . \end{aligned} \tag{34}$$

Thus, Q_{lop} is equal to the standard Q parameter $= \kappa c/\pi G\mu_{\mathrm{un}}$ (Toomre 1964; Jog & Solomon 1984a) for the axisymmetric case; divided by f_μ.

From the variation in f_μ with ϕ (§ 2.7), it can be seen that the region $\phi = 0°$–$90°$ and $\phi = 270°$–$360°$ would show lower values of Q_{lop} than the axisymmetric case, indicating a more unstable disk, whereas the reverse is true for the region $\phi = 90°$ to $270°$. The Q_{lop} value is lowest in a region of maximum overdensity, that is at $\phi = 0°$, indicating the most unstable region at a given radius.

Since the gas density would also be affected in the same fashion, the Q_{lop} values for gas also would have a similar dependence on ϕ. Hence the gravitationally coupled two-fluid stars plus gas system (Jog & Solomon 1984a, 1984b; Jog 1996) would also be more unstable in regions of high

surface densities. This can further decrease the stability of the gas. The azimuthal variation in $Q_{\rm lop}$ results in asymmetric star formation (see § 3.3).

3.2.1. $Q_{\rm lop}$ *Values for Gas in Lopsided Galaxies*

Here we apply the $Q_{\rm lop}$ criterion for the local stability in a lopsided disk (eq. [34]) to gas in some galaxies showing an asymmetric gas distribution in the inner regions, namely M101 and NGC 4565. Since the observed values of A_1/A_0 are important at $R \geq 2.5R_{\rm exp}$ (§ 2.2), we obtain the $Q_{\rm lop}$ values at this radius. The aim is to show that since the gas in a typical galactic disk is close to $Q = 1$, corresponding to the threshold for star formation (Kennicutt 1989), even a small increase in the gas surface density in the overdense region in a lopsided galaxy can lead to the formation of stars.

For M101, Kenney et al. (1991) obtain $R_{\rm exp} = 3.1$ kpc and detect H_2 up to 7 kpc, which is only slightly smaller than $2.5R_{\rm exp} = 7.5$ kpc. At this radius, the observed rotation velocity is $\sim$220 km s^{-1} with a nearly flat rotation curve, and the observed values of the H I and H_2 surface densities are 6 and 4 $M_\odot$ pc^{-2}, respectively, giving the total gas density of 10 $M_\odot$ pc^{-2}. The random velocity for gas, c, in galaxies is observed to be a robust quantity, and we take its value to be 5 km s^{-1} (Jog & Ostriker 1988). Hence the value of the standard (axisymmetric) Q for gas is calculated to be 1.4. The values of A_1/A_0 for M101 have not been measured yet but are probably high $\sim$0.3–0.4 (see § 2.2). For these values the minimum $Q_{\rm lop}$ (at $\phi = 0°$; see eq. [34]) for gas is obtained to be 1.1 and 0.9, respectively. Thus, on taking account of the effective increase in the surface density in the overdense region in a lopsided potential, the gas becomes *unstable*, whereas it was stable in the axisymmetric case. This can lead to an enhanced star formation (§ 3.3).

For NGC 4565, the total (H I + $2H_2$) column density at $2.5R_{\rm exp} = 5'$ is $\sim$17 $M_\odot$ pc^{-2} (Richmond & Knapp 1986), and the rotation curve is flat with a velocity of 255 km s^{-1} (Rupen 1991). The axisymmetric Q-value for gas is calculated to be 0.6, which is already less than 1; hence, any enhancement of surface density in the overdense regions would make the gas more unstable.

It is interesting that the other galaxies in the BLS sample showing a substantial asymmetry in H I at large radii do not show a significant asymmetry in the gas at low radii, see for example NGC 2841 (Young & Scoville 1982b), NGC 891 (Scoville et al. 1993), and IC 342 (Sage & Solomon 1991). We would also like to estimate $Q_{\rm lop}$ values for galaxies with high A_1/A_0 values in the RZ sample, but unfortunately there are no CO data in the literature for these galaxies.

3.3. *The Asymmetry in the Distribution of* H II *Regions*

The observed azimuthally asymmetric distribution of H II regions in say, M101 (see § 1.2) can be explained naturally from the results for an azimuthal variation in H_2 gas density (§§ 2.7, 3.1) and the local stability (§ 3.2) in a lopsided potential. The molecular hydrogen gas is known to be the site of star formation, and it is shown to be distributed asymmetrically (§ 3.1) with an enhanced fraction in the azimuthal range of $\phi = 0°$–$90°$ and $\phi = 270°$–$360°$. As a result of the increase in the effective surface density, the corresponding $Q_{\rm lop}$ value for gas would be lowered in this region and could become ≤ 1 even if it was greater than one in an azimuthally symmetric galaxy (see § 3.2). A necessary and sufficient condition for the onset of star formation (Quirk 1972; Kennicutt 1989) has often been proposed to be Q for gas be less than 1. The mechanism for cloud-cloud collisions leading to a higher rate of massive star formation (Scoville, Sanders, & Clemens 1986) would also give a higher star formation rate in a region of higher surface density. Hence we predict a higher star formation rate to occur in the overdense regions in lopsided galaxies.

Further, we argue that the star formation in a region of high surface density would result in a higher fraction of massive star formation since there is a good coupling between the dust and the gas; thus, the gas temperature is higher, which results in a higher critical/minimum value for the mass of the stars formed (Larson 1986; Jog & Solomon 1992). The massive stars would evolve into H II regions, and thus we predict the number of H II regions to be asymmetrically distributed in lopsided galaxies with a higher fraction seen in regions of higher surface densities. In contrast, the gas is more stable in the underdense region than in the axisymmetric case. This would lead to a lower star formation rate and thus further contribute to the overall asymmetry seen in the H II regions across the disk. Since the isophotes are elongated in the direction where the effective surface density is highest (§ 2.7), we predict more H II regions in the elongated regions of isophotes, which agrees with observations for M101. The asymmetry in H_2 distribution is shown to be even higher in large, late-type galaxies (§ 3.1), which will then contribute to a more asymmetric distribution of H II regions in such galaxies.

If the phase of the lopsided potential, $Q_{\rm lop}(R)$, is constant with radius as is typically observed (§ 2.6), the density would be higher in one-half of the lopsided galaxy while the other half would be underdense (§ 2.7). Hence the resulting H II region formation would be higher in one-half of the galaxy, as discussed above. If, on the other hand, $\phi_{\rm lop}(R)$ shows a variation with radius, then the intensity contours will appear to be a one-armed spiral (§ 2.6), and the resulting H II region distribution will also show a similar trend. This explains why the observed number of H II regions is higher near the $m = 1$ old stellar southern arm of NGC 2997 (Block et al. 1994). In the literature, there are good studies of observed radial variation in the number density and other properties of H II regions in galaxies (Hodge & Kennicutt 1983; Athanassoula, Garcia-Gomez, & Bosma 1993). Similar high-quality systematic studies of *azimuthal* variation of H II regions in galaxies are needed. This will allow a better comparison of our results with observations.

The luminosities of H II regions in M101 and NGC 628 are much higher than in the Galaxy (Kennicutt, Edgar, & Hodge 1989). The large gas densities increase the probability of having self-propagating star formation (Seiden 1983), and this could lead to the formation of giant, combined H II regions. This may be the reason why the net luminosities of H II regions in lopsided galaxies are higher.

4. DISCUSSION

4.1. *The Nondisk (Halo) Origin of the Lopsided Potential*

The logarithmic potential ψ_0 used for the unperturbed disk (eq. [7]), and the exponential form used for the unperturbed surface density (eq. [12]) are not internally self-consistent in that they do not obey the Poisson equation (e.g., Freeman 1970). The treatment in § 2 is, however, still valid if the net potential ψ_0 in the disk is contributed by the disk, halo, and the bulge components.

Further, the lopsided potential and the disk response are shown to be anticorrelated (§ 2.7). Thus, the treatment in this paper and in RZ to calculate the A_1/A_0 values by matching the perturbed exponential surface density by a $m = 1$ distribution is valid if the lopsided disk potential is assumed to be caused by a perturbation in the halo rather than in the disk. If the halo is responsible for ψ_{lop}, then one can have only the density response in the disk, and this would correspond to the observed $m = 1$ disk amplitude. An indirect proof for the halo being the source of the lopsided potential comes from the fact that ϵ_{lop} is observed to increase with radius, and it is known that the halo has an increasing dominance in the galaxy dynamics at large radii. For the particular case of the Milky Way, Weinberg (1995) has shown that its halo is distorted due to the tidal interaction with the Magellanic Clouds, and galactic disk then responds to this halo lopsided potential.

4.2. *Asymmetry of Atomic Hydrogen Gas at Large Radii*

In this paper, we only study the asymmetry in the stars and gas in the inner/optical regions of a galaxy. We do not study the asymmetry of H I at large radii. In some galaxies, the asymmetry in the H I gas at large radii is along the same direction as the asymmetry in H I and H_2 in the inner/optical disk as observed, for example, in NGC 4565 (Richmond & Knapp 1986; Rupen 1991) and in NGC 628: compare the H_2 observations (Adler & Liszt 1989) with the H I observations (Kamphuis & Briggs 1992). Or, in contrast, in some galaxies the isodensity contours for H I in the outer regions are more elongated in a direction opposite to the extent of H I and H_2 in the inner regions, as seen, for example, in M101 (Bosma et al. 1981, Kenney et al. 1991) and in IC 342 (Newton 1980; Sage & Solomon 1991). This can be understood in terms of the non-disk (halo) origin of the lopsided potential (§ 4.1). Galaxy interaction (Weinberg 1995) has been proposed as the cause of the halo lopsided potential. If a galaxy were to undergo two or more subsequent encounters of different orientations and strengths, it can generate global perturbations in the halo mass distribution which may be along different directions in different radial regions. Thus the gas asymmetry in the outer regions of a particular galaxy may or may not be correlated with that in the inner regions.

Further, the H I gas lying in outer regions is more susceptible to perturbation due to a tidal interaction with galaxies, or accretion of high-velocity clouds as seen for M101 (Van der Hulst & Sancisi 1989) or even an interaction with an intergalactic medium as seen in the Virgo cluster galaxy NGC 4654 (Phookun & Mundy 1995). Hence we do not discuss the extended H I distribution.

4.3. *Extremely Large Values of A_1/A_0 and Starbursts in Mergers*

Extremely lopsided mass distribution seems to occur in strongly disturbed galaxies with ongoing mergers or that have undergone a recent merger such as NGC 3921. These are also characterized by "E + A spectra" (Schweizer 1996) where both the starburst and the lopsided phenomena are presumably triggered by the strong galaxy interactions. It is not clear if the assumption of an average exponential surface density is valid for such strongly perturbed galaxies. But if it is, and if the A_1/A_0 values are observed, then we can explain the resulting starbursts in the overdense regions of these galaxies. This would be an extreme case of the enhanced H II region formation discussed in § 3.3. An additional mechanism for star formation in this case could be a starburst due to the shock compression of the pre-existing molecular clouds via the overpressure of remnants of colliding H I clouds from the two colliding galaxies as was proposed by Jog & Solomon (1992).

5. CONCLUSIONS

We study the dynamics of particles on closed orbits in a galactic disk perturbed by a lopsided halo potential and obtain the azimuthal variation in the effective surface density for an exponential disk. The results are obtained first for a disk with a flat rotation curve and then also for a general power-law rotation curve. These results are shown to be valid for both stars and gas in the inner (optical) regions because both respond to the same lopsided potential and have comparable disk scale lengths. The azimuthal variation in gas density is shown to affect the local gas stability, and this leads to an azimuthally asymmetric star formation. The main conclusions from this paper are summarized below:

1. An orbit is shown to be elongated along the minimum in the lopsided potential, and shortened along the opposite direction. The net rotational velocity is shown to be highest at the minimum radial extent of the orbit.
2. The parameter ϵ_{lop} denoting the small perturbation in the potential is obtained as a function of A_1/A_0, the observed fractional amplitude of the $m = 1$ azimuthal Fourier component of the surface brightness and the radius. The typical value of ϵ_{lop} is obtained to be a few percent, and the values increase with radius.
3. The value of ϵ_{iso}, the ellipticity of an isophote is shown to be higher than ϵ_{lop} by at least a factor of 4. This explains why the phenomenon of lopsidedness is so commonly detected. Second, the high value of this ratio means that even for the strongly visually lopsided galaxies which may have $A_1/A_0 \sim 0.4$; the potential is still fairly axisymmetric with a small $\epsilon_{lop} \sim 0.07$. Thus such galaxies are still dynamically robust.
4. The effective surface density is highest along the maximum in the lopsided potential and there is an underdense region along the opposite direction.
5. If the phase of the lopsided potential is constant with radius as is typically observed for strongly lopsided galaxies, then the isophotes for an $m = 1$ distribution will be aligned egg-shaped ovals, as seen in M101 and NGC 1637. If the phase varies with radius, the isophotes will show a prominent one-armed spiral structure as seen in M51 and NGC 2997.
6. The isophotes are elongated along the direction where the effective surface density is highest. This agrees with the observations of M101. Future two-dimensional maps of CO and H I (in inner regions) of other galaxies can further check this result.
7. We obtain the local stability parameter Q_{lop} in a lopsided galaxy and calculate its values for gas in lopsided galaxies for which the data for the total gas density are available. The Q_{lop} values are shown to be significantly lowered compared to the axisymmetric case in the overdense regions.
8. The lowering of Q_{lop} values to ≤ 1 in regions of high surface densities is argued to result in an enhanced rate of formation of massive stars and hence H II regions. Thus we

can naturally explain the observed azimuthal asymmetry in the distribution of the H II regions in the lopsided galaxies such as M101 (§ 3.3).

Due to the higher self-shielding of gas in regions of high density, the asymmetry in the distribution of the molecular hydrogen gas and the resulting H II regions is argued to be higher in the large, late-type galaxies.

9. We suggest that future observational studies should present the full azimuthal distribution of the H_2 and H I gas surface densities, and also the H II regions, especially for clearly lopsided galaxies. This would allow a better comparison of predictions from our model and would lead to a better understanding of gas dynamics and star formation in lopsided galaxies.

I thank the referee, Albert Bosma, for many thoughtful and constructive comments, and particularly for raising the issues of the phase of the $m = 1$ isophotes and the distinction in the gas asymmetry between the inner versus outer regions.

REFERENCES

Adler, D. S., & Liszt, H. S. 1989, ApJ, 339, 836
Allen, R. J. 1975, in CNRS Coll. 241, la Dynamique des Galaxies Spirales, ed. L. Weliachew (Paris: CNRS), 157
Arp, H. 1966, ApJS, 14, 1
Athanassoula, E., Garcia-Gomez, C., & Bosma, A. 1993, A&AS, 102, 229
Baldwin, J. E., Lynden-Bell, D., & Sancisi, R. 1980, MNRAS, 193, 313 (BLS)
Beale, J. S., & Davies, R. D. 1969, Nature, 221, 531
Binney, J., & Tremaine, S. 1987, Galactic Dynamics (Princeton: Princeton Univ. Press)
Block, D. L., Bertin, G., Stockton, A., Grosbol, P., Moorwood, A. F. M., & Peletier, R. F. 1994, A&A, 288, 365
Bosma, A. 1978, Ph.D. thesis, University Groningen
Bosma, A., Goss, W. M., & Allen, R. J. 1981, A&A, 93, 106
Casertano, S., & Van Gorkom, J. 1991, AJ, 101, 1231
Duley, W. W., & Williams, D. A. 1984, Interstellar Chemistry (London: Academic)
Earn, D. J. D., & Lynden-Bell, D. 1996, MNRAS, 278, 395
Franx, M., & de Zeeuw, T. 1992, ApJ, 392, L47
Freeman, K. C. 1970, ApJ, 160, 811
Gerhard, O. E., & Vietri, M. 1986, MNRAS, 223, 377
Hodge, P. W., & Kennicutt, R. C. 1983, ApJ, 267, 563
Jog, C. J. 1992, ApJ, 390, 378
———. 1996, MNRAS, 278, 209
Jog, C. J., & Ostriker, J. P. 1988, ApJ, 328, 404
Jog, C. J., & Solomon, P. M. 1984a, ApJ, 276, 114
———. 1984b, ApJ, 276, 127
———. 1992, ApJ, 387, 152
Junqueira, S., & Combes, F. 1996, A&A, 312, 703
Kamphuis, J., & Briggs, F. 1992, A&A, 253, 335
Kenney, J. D. P., Scoville, N. Z., & Wilson, C. D. 1991, ApJ, 366, 432
Kennicutt, R. C. 1989, ApJ, 344, 685
Kennicutt, R. C., Edgar, R. K., & Hodge, P. W. 1989, ApJ, 337, 761
Kuijken, K. 1993, ApJ, 409, 68
Kuijken, K., & Tremaine, S. 1994, ApJ, 421, 178
Larson, R. B. 1986, in Stellar Populations, ed. C. A. Norman, A., Renzini, & M. Tosi (Cambridge: Cambridge Univ. Press), 101
Lord, S. D., & Young, J. S. 1990, ApJ, 356, 135
Mihalas, D., & Binney, J. J. 1981, Galactic Astronomy (San Francisco: Freeman)
Newton, K. 1980, MNRAS, 191, 169
Phookun, B., & Mundy, L. G. 1995, ApJ, 453, 154
Phookun, B., Vogel, S. N., & Mundy, L. G. 1993, ApJ, 418, 113
Quirk, W. J. 1972, ApJ, 176, L9
Richmond, M. W., & Knapp, G. R. 1986, AJ, 91, 517
Richter O.-G., & Sancisi, R. 1994, A&A, 290, L9
Rix, H.-W. 1996, in IAU Symp. 169, Unsolved Problems Of The Milky Way, ed. L. Blitz & P. Teuben (Dordrecht: Kluwer), 23
Rix, H.-W., & Rieke, M. J. 1993, ApJ, 418, 123
Rix, H.-W., & Zaritsky, D. 1995, ApJ, 447, 82 (RZ)
Rogstad, D. H. 1971, A&A, 13, 108
Rohlfs, K. 1977, Lecture Notes in Physics, Vol. 69, Lectures On Density Wave Theory (Berlin: Springer-Verlag)
Rubin, V. C., Ford, W. K., & Thonnard, N. 1978, ApJ, 225, L107
Rubin, V. C., Whitmore, B. C., & Ford, W. K., Jr. 1988, ApJ, 333, 522
Rupen, M. P. 1991, AJ, 102, 48
Sage, L. J., & Solomon, P. M. 1991, ApJ, 380, 392
Sakamoto, S., & Hasegawa, T. 1997, in preparation
Sancisi, R. 1981, in The Structure and Evolution of Normal Galaxies, ed. S. M. Fall & D. Lynden-Bell (Cambridge: Cambridge Univ. Press), 149
Sandage, A. 1961, The Hubble Atlas of Galaxies (Washington: Carnegie Inst. Washington)
Schechter, P. L. 1996, in IAU Symp. 169, Unsolved Problems Of The Milky Way, ed. L. Blitz & P. Teuben (Dordrecht: Kluwer), 633
Schweizer, F. 1996, AJ, 111, 109
Scoville, N. Z., & Sanders, D. B. 1987, in Interstellar Processes, ed. D. J. Hollenbach & H.A. Thronson (Dordrecht: Reidel), 21
Scoville, N. Z., Sanders, D. B., & Clemens, D. P. 1986, ApJ, 310, L77
Scoville, N. Z., Thakkar, D., Carlstrom, J. E., & Sargent, A. I. 1993, ApJ, 404, L59
Seiden, P. E. 1983, ApJ, 266, 535
Sellwood, J. A., & Merritt, D. 1994, ApJ, 425, 530
Shaya, E., & Federman, S. 1987, ApJ, 319, 76
Solomon, P. M., Barrett, J., Sanders, D. B., & de Zafra, R. 1983, ApJ, 266, L103
Symon, K. R. 1960, Mechanics (Reading: Addison-Wesley)
Toomre, A. 1964, ApJ, 139, 1217
Van der Hulst, J. M., & Sancisi, R. 1988, AJ, 95, 1354
Weinberg, M. D. 1995, ApJ, 455, L31
Wevers, B. M. H. R., van der Kruit, P. C., & Allen, R. J. 1986, A&AS, 66, 505
Young, J. S., & Scoville, N. Z. 1982a, ApJ, 258, 467
———. 1982b, ApJ, 260, L41
———. 1991, ARA&A, 29, 581
Young, J. S., et al. 1995, ApJS, 98, 219
Zaritsky, D., & Rix, H.-W. 1997, ApJ, 477, 118